IEEE Access
Multidisciplinary | Rapid Review | Open Access Journal

Received January 27, 2021, accepted February 16, 2021, date of publication February 24, 2021, date of current version March 5, 2021.

Digital Object Identifier 10.1109/ACCESS.2021.3061913

Impact of the Generation Interval on the Performance of Sidelink C-V2X Autonomous Mode

STEFANIA BARTOLETTI[1,2], (Member, IEEE), BARBARA MAVÌ MASINI[1,2], (Senior Member, IEEE), VINCENT MARTINEZ[3], IOANNIS SARRIS[4], AND ALESSANDRO BAZZI[2,5], (Senior Member, IEEE)

[1]Institute of Electronics, Computer and Telecommunication Engineering of CNR (IEIIT-CNR), 40136 Bologna, Italy
[2]CNIT/WILAB, 40136 Bologna, Italy
[3]NXP Semiconductors, 31023 Toulouse, France
[4]u-blox Athens, 15125 Athens, Greece
[5]DEI, Università di Bologna, 40136 Bologna, Italy

Corresponding author: Alessandro Bazzi (alessandro.bazzi@unibo.it)

ABSTRACT Cellular-vehicle-to-everything (C-V2X) is gaining an increasing interest among the technologies under consideration for future connected and automated vehicles, especially for sidelink LTE-V2X Mode 4 and sidelink 5G-V2X Mode 2, where nodes autonomously perform resource allocations and transmissions, without relying on any infrastructure. In these cases, the allocation process has been designed based on the assumption of periodic packet generation constrained to a few possible allocation periods. Nevertheless, even assuming that the awareness messages are continuously exchanged, the packet generation might not always be exactly periodical or might come with a periodicity not constrained to the expected values, as for example with the Cooperative Intelligent Transport Systems (C-ITS) standard defined by the European Telecommunications Standards Institute (ETSI). The non-ideal periodicity of packet generation, if not properly taken into account, can significantly impact the operation and performance of C-V2X when vehicles autonomously select their radio resources. This paper provides an analysis of how a misalignment between packet generation and resource allocation affects the system performance and provides insights into how to design the parameter settings to improve the performance. A case study is provided, focusing on LTE-V2X Mode 4 and the cooperative awareness message (CAM) generation in agreement with the the ETSI specifications. Results show that the performance generally improves if the smallest allocation interval is adopted and if the reservation is maintained even when no packets are ready for transmission. It is also shown how the parameter controlling the maximum latency in LTE-V2X, jointly with the misalignment between the allocation and generation intervals, can further affect the packet reception rate.

INDEX TERMS LTE-V2X, 5G-V2X, sidelink, connected vehicles, autonomous resource allocation.

I. INTRODUCTION

The transport systems and the automotive industries are undergoing key technological transformations since an increasing number of connected and automated vehicles is populating our roads, providing enhanced safety and efficiency. In this landscape, vehicle-to-everything (V2X) connectivity, enabling vehicles to cooperate with one another, with roadside infrastructures, with pedestrians and with the other road elements, will improve the awareness and the perception of the scenario.

Sidelink LTE-V2X and sidelink 5G-V2X are two access layer technologies developed under the umbrella of cellular-V2X (C-V2X) and standardized by the 3GPP as access layer replacement for IEEE 802.11p. These C-V2X access layers are investigated for application in ITS stacks and related protocols, such as ETSI ITS in Europe. LTE-V2X was included in Release 14 of 4G as an evolution of device-to-device (D2D)

The associate editor coordinating the review of this manuscript and approving it for publication was Walid Al-Hussaibi.

initially imagined for public safety applications in Release 12 [1]–[5]. 5G-V2X is instead still under definition in Release 17 (the last part of the standardization is expected in 2022), based on the new radio (NR) of 5G [6]–[11], aimed at providing new capabilities and stringent quality of service (QoS) requirements for a more secure and smarter operation [12]–[15].

In 4G and 5G, two transmission modes support direct V2X communications, both transmitting in the sidelink channel over the PC5 interface, but differing on how radio resources are allocated [16]–[19]. In the first one (Mode 3 in LTE-V2X and Mode 1 in 5G-V2X), the resource selection, allocation, and reservation is performed by the network and commanded via the Uu interface to the nodes, which must be within the coverage of the cellular network. In the other one (Mode 4 in LTE-V2X and Mode 2 in 5G-V2X), the resources are autonomously selected by the stations, based on some local sensing mechanism, therefore allowing the vehicles to communicate even in out-of-coverage conditions. Once selected, the resources are used periodically for a certain time, and then a new resource selection is performed, i.e. through a procedure called *resource reselection*. According to [20], the centralized perspective of Mode 3 provides, in principle, more information to the scheduler resulting into a performance improvement. However, it poses non-negligible challenges in several conditions, such as at the cell edge (where outage can occur), in multi-operator (handover) scenarios and when high vehicle density is addressed. Beside these, it must be highlighted that V2X safety applications should be ubiquitous and cannot depend on the availability of an infrastructure-based cellular coverage. Thus, the autonomous mode plays a key role.

In the sidelink LTE-V2X autonomous mode, vehicles independently select their radio resources through a distributed scheduling protocol, namely the sensing-based semi-persistent scheduling (SB-SPS). Such a protocol assumes a periodic nature of the exchanged physical layer messages, estimates the occupied resources in the last period of time, predicts the future use of resources and then performs a semi-persistent reservation of the identified resources for a given period. Even if extended with new features, the basic operations are expected to be maintained in 5G-V2X.

The rationale for assuming periodic messages in the design of the resource allocation mechanisms is that V2X Day 1 applications[1] are based on the exchange of messages, which are continuously sent by each vehicle in broadcast. Such messages, called cooperative awareness messages (CAMs) in Europe, defined by the ETSI, and basic safety messages (BSMs) in the US, defined by the Society of Automotive Engineers (SAE), contain updates about the state and movements of the vehicle. Indeed, these and most of the messages that are currently under definition, such as the ETSI collective perception messages (CPMs) and vulnerable road user awareness messages (VAMs), have a repetitive nature and are in some specific cases periodic.

However, as detailed in further sections, focusing on CAMs as a case study and in order to better cope with the trade-off between timeliness and channel load, they tend to have adaptive generation intervals and are thus in general not periodic [21]: on the one hand, an higher beacon generation frequency is desirable in case of high speed, when the vehicle information needs to be updated more often; on the other hand, a lower message generation frequency, reducing the channel occupation and the collision probability, is preferable in low speed scenarios. Additionally, even when the packet generation is periodic, this periodicity might not be the same as the SB-SPS algorithm periodicity; whereas the packet generation is in fact designed without particular limitations, the periodicity of resource allocation is instead constrained by the time structure of LTE-V2X and 5G-V2X, which is based on a subframe length of either 0.25 ms, 0.5 ms, or 1 ms (the last one in LTE and any of the three in 5G, depending on the NR subcarrier spacing). The mismatch between the packet generation frequency and the periodicity of resource allocation can lead to inefficient allocations and major packet losses. Therefore, the proper set of system parameters cannot always rely on the assumption of exact periodicity and must be able to cope with a possible misalignment.

In this paper, we investigate the effect of a mismatch between the packet generation frequency at upper layers of the ITS stack and the allocation periodicity at physical layer in sidelink C-V2X autonomous mode, with reference, as a case study, to sidelink LTE-V2X Mode 4 (simply referred as LTE-V2X in the rest of the paper) and to the speed-dependent triggering mechanisms of CAMs as specified by ETSI [22]. We show a system level analysis performed via simulations under various traffic densities and vehicle speeds. The key contributions of the paper can be summarized as follows:

- We clarify how the allocation period and generation frequency interrelate and influence sidelink C-V2X autonomous mode;
- We derive a model to calculate the average number of reselections for a vehicle moving at a constant speed as a function of several parameters;
- We provide system-level results to analyze the performance of sidelink LTE-V2X Mode 4 varying the generation frequency, vehicle speed, and vehicle densities; and
- We identify general guidelines for the setting of those parameters and procedures which are not constrained by specifications and mostly affect the system performance.

The remainder of the paper is organized as follows. Section II describes the related work and state-of-the-art. Section III introduces LTE-V2X Mode 4 and 5G-V2X Mode 2. Section IV deals with the European protocol stack, the specific case of the generation of CAM messages and the relationship between message generation and packet

[1]Day 1, Day 2, and Day 3+, indicate the sequence of deployment phases following Car-to-Car Communication Consortium (C2C-CC) from dissemination of local status information and warnings to cooperative automated driving.

transmission in LTE-V2X. Section V presents a case study with system level results. Finally, Section VI gives our conclusions.

II. RELATED WORK AND PAPER SCOPE

The first version of LTE-V2X was completed within 3GPP Release 14 in 2017, followed by refinements in Release 15. 5G-V2X is instead addressed through Releases from 15 to 17: the main applications and requirements are identified in Release 15; the first set of specification is introduced in Release 16, mainly dealing with architecture and physical layer; finally, 5G-V2X will be completed, with details on the access procedures, in Release 17, which is still under discussion.

Since its first introduction, attention has been posed to address the performance of LTE-V2X in general [5], [20], [23] or in comparison with IEEE 802.11p/ITS-G5 [24], [25]. A large number of papers have also investigated some specific aspects. Just as few examples, the use of network coding is proposed in [26] (raptor Q coding) and [27] (index-coding), and the exploitation of exponentially weighted measurements of the received power rather than simple average is suggested in [28]. Efficient scheduling and resource allocation have been also widely addressed for LTE-V2X in last few years, especially with the objective to optimize the resource allocation, as in in [29]–[31], improve the channel occupancy, as in [32], or provide the expected QoS, as in [33].

The 5G-V2X technology is instead under definition and, as a consequence, still less investigated. In [8], a first description of the features under development in 5G-V2X is provided, in [9], a link-layer performance comparison with the other solutions (IEEE 802.11p, IEEE 802.11bd, and LTE-V2X) is shown, and in [34] first investigations on novel semi-distributed transmission paradigms are proposed.

All the mentioned works have as a common simplifying hypothesis the use of a packet generation interval exactly equal to the allocation periodicity applied by either LTE-V2X or 5G-V2X access layers. Also in [35], [36], where congestion control is investigated and variable packet generation is considered, the issue of the mismatch between packet generation and resource allocation periodicity is not deepened. In [35], the generation interval is kept fixed and the effect of congestion control is rather to discard some packets at the higher layers. In [36], various generation periods are compared but always assuming the same value as allocation periodicity.

A packet generation interval exactly equal to the allocation periodicity, which is acceptable for general considerations and even correct under specific circumstances, is not expected to be always valid for many types of messages that are already defined or that are currently under definition. As the main example, also better discussed in Section III, CAM messages are generated depending on the dynamics of the vehicle and are not periodic in most of the cases. This is for example remarked in [21], where the authors analyze the CAM messages recorded by two car manufacturers during experiments performed on field in urban, sub-urban and highway test drives. In [21], it is shown that both the size of the messages and the time interval between consecutive CAMs are largely variable in time. The authors also derive a model for the generation of realistic messages in simulators.

A very few works do not rely on this assumption. In [37], where the feasibility of implementing the distributed congestion control algorithm specified in SAE J2945/1 standard on top of the C-V2X stack is investigated, the packet inter-arrival time is indeed adapted to the estimated congestion level, thus in principle causing a mismatch with the allocation period; however, how the authors deal with this is not detailed and the consequences are not analyzed from this point of view. More relevantly, based on the model presented in [21], a comparison of ITS-G5 and sidelink LTE-V2X is proposed in [38]. Taking into account a realistic generation of the CAMs, it is observed that LTE-V2X suffers of variable size and variable generation intervals, whereas ITS-G5 is inherently not impacted by these effects. Finally, in [39] the authors investigate the impact of aperiodic traffic, assuming the inter-packet distance following an exponential distribution. In their work, they observe that treating each packet as a new sporadic transmission is preferable than using periodical allocations and dropping packets when a resource is not available or randomly choosing a new one when needed.

In this work, we specifically focus on the impact of a mismatch between the packet generation interval and the allocation periodicity. Differently from previous works, the scope is here to elaborate on the implications in LTE-V2X of such mismatch. We provide a systematic investigation, clarifying which are the options possible at the implementation, and identifying the ways the scheduler can be configured to better cope with this issue.

III. RESOURCE ALLOCATION IN LTE-V2X MODE 4 AND 5G-V2X MODE 2

In this section, a brief description of LTE-V2X and 5G-V2X is provided, taking into account that the standardization process for 5G-V2X is not concluded. Only the main aspects will be here recalled and more details can be found for example in [8], [9], [40].

A. PHYSICAL LAYER OF LTE-V2X AND 5G-V2X

At the lower layers, sidelink numerology and building blocks of LTE-V2X and 5G-V2X are based on uplink, which is single carrier frequency division multiple access (SC-FDMA) in LTE-V2X and cyclic prefix orthogonal frequency-division multiple access (CP-OFDM) in 5G-V2X. LTE-V2X operates in 10 MHz or 20 MHz channels, whereas 5G-V2X can occupy up to 100 MHz when used in bands below 6 GHz (namely, sub 6 GHz). The resources are based on a time-frequency matrix structure: the time domain is divided into transmission time intervals (TTIs), of 1 ms duration in LTE-V2X and of either 0.25 ms, 0.5 ms, or 1 ms in 5G-V2X (sub 6 GHz); the frequency domain is organized in sub-channels, in turn

composed of a certain number of subcarriers (spaced by 15 kHz in LTE and 15, 30, or 60 kHz in 5G). Multiple modulation and coding schemes (MCSs) are possible in both technologies.

There are two main PHY channels used to transmit the packets: i) the Physical Sidelink Shared channel (PSSCH) for data packets, also called transport blocks (TBs); and ii) the Physical Sidelink Control Channel (PSCCH) for the associated control information, also known as sidelink control information (SCI), which carries the information that the receiving stations requires to be able to receive and demodulate the PSSCH. The SCI is sent during the same TTI as the data, independently to the vehicle speed and for both LTE and 5G.

Additionally, the physical sidelink feedback channel (PSFCH) is added in 5G NR V2X to allow the receiver sending positive and negative acknowledgment. The TB and the associated SCI are transmitted in the same TTI. The transmission of one TB is performed in a single TTI and a number of adjacent sub-channels which depends on the packet size and the adopted MCS.

B. LTE-V2X MODE 4 ALLOCATION PROCEDURE

LTE-V2X Mode 4 was firstly defined in Release 14. In Mode 4, each station autonomously identifies the resources to allocate employing a SB-SPS. First of all, a parameter T_b is set to define the periodicity for resource allocation. T_b can be chosen equal to 20 ms, 50 ms, or any multiple of 100 ms up to 1 s [41]. When the first allocation is performed, starting from the interval T_b and the number of subchannels required to transmit the given message, the station defines a grid of possible allocations in the next T_b called candidate single-subframe resource (CSSR). In order to estimate the future occupation of the CSSRs, the station uses the power measured in each subchannel and the content of the received SCIs during a sensing window of $T_{sense} = 1$ s. The SCIs include an indication about the selected and reserved sub-channels by the neighboring stations. Among the CSSRs that are assumed available, the 20% which received less interference in T_{sense} is passed to the medium access control (MAC) layer, which randomly selects the one to be used. Possibly, two parameters denoted as T_1 and T_2 can be used by the higher layers to set a minimum and maximum delay, respectively, between the message generation and its transmission. T_2, in particular, can be used to guarantee a given QoS in terms of latency. The latency requirements are application-dependent. For example, safety-related use cases are expected to have very stringent requirements. In most of the cases, the latency deadline for CAMs is set to be equal or lower than 100ms.

Once selected, the same CSSR is kept periodically, with periodicity T_b, for a certain time; this process is called SB-SPS and has been introduced to avoid the need for frequent changes of the resource selection, also called reselections. More specifically, the allocation is kept for a random number of periods, for example uniformly selected between 5 and 15 when $T_b = 100$ ms. After that time, the same resource is still maintained with probability p_k, which is a parameter set by the operator between 0 and 0.8. The SB-SPS is a key mechanism in order to let the other nodes estimating the future occupation and thus reduce packet collisions but is also prone to possible long bursts of errors [42].

The allocation process is exemplified in Fig. 1. Four subchannels are supposed in the example and the allocation period T_b lasts six TTIs. Assuming one packet occupies one subchannel, this means that there are $4 \times 6 = 24$ possible CSSRs. The sensing interval during which the power is measured and SCIs are decoded is denoted as T_{sense} and includes in the example three times T_b, thus the power associated to each of the 24 CSSRs is the average of three values. The average power cannot be estimated in those TTIs in which the node is transmitting, due to the half-duplexing nature of current radios. The station selects a set of candidate resources from a selection window delimited in time by T_1 (here excluding for example the first TTI) and T_2 (here excluding for example the last TTI).

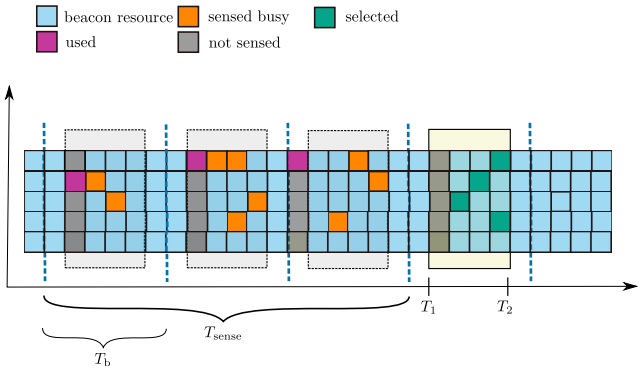

FIGURE 1. Illustration of the SB-SPS. The sensing period is indicated as T_{sense} and contains three allocation periods. In the example, the frequency domain contains five BRs per subframe and each allocation period contains six subframes. The candidates passed to the MAC layer are found in the allocation period delimited by T_1 and T_2.

C. WHAT IS EXPECTED IN 5G-V2X MODE 2

The autonomous allocation procedure in 5G-V2X is called Mode 2 and, differently from LTE-V2X Mode 4, is split into several sub-modes [43]: Mode 2a is expected to inherit the same procedure of LTE-V2X Mode 4; Mode 2b was initially set to allow the stations assisting their neighbors in performing resource selection; this feature was later considered helpful in addition to other sub-modes and thus removed as a specific sub-mode; Mode 2c allows to specify a given pattern instead or in addition to the sensing procedure, so that with predefined allocations it is in principle possible to enable very low latency and very reliable transmissions for specific applications; Mode 2d allows a station to select and allocate resources for other stations, which is particularly helpful when vehicles are grouped such as in platoons.

Other relevant aspects of 5G-V2X are the addition of unicast and groupcast transmissions (only broadcast is possible in LTE-V2X), the already mentioned feedback channel

to provide positive and negative acknowledgments, and a short-term sensing for non-periodical transmissions.

For the purpose of this paper it is to note that, despite the various additional features expected in 5G-V2X, still the SB-SPS allocation based procedure initially designed in Release 14, now called Mode 2a, is expected to be the main one to deal with recurrent messages similar to CAMs.

IV. RELATIONSHIP BETWEEN MESSAGE GENERATION AND PACKET TRANSMISSION IN LTE-V2X

LTE-V2X and 5G-V2X are intended as possible options for the access layers of protocol pillars that were initially defined with other technologies in mind. The European solution, which is the one considered in this paper, is defined by ETSI under the name of cooperative-intelligent transport systems (C-ITS).

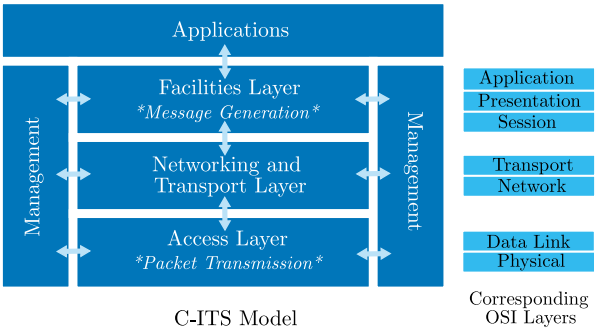

FIGURE 2. ETSI C-ITS-S architecture.

In Fig. 2, the architecture of the so-called C-ITS station (C-ITS-S) is reported, as defined in [44]. As observable, the protocol pillar includes three main layers in the middle of the figure: the *facilities layer*, which basically covers the session, presentation, and application layers of the OSI model; the *transport and network layer*, which corresponds to the two OSI layers bringing the same names; the *access layer*, which focuses on the data link (including MAC) and physical (PHY) OSI layers. In addition, *management* and *security* layers are foreseen as cross-layer entities, and applications are seen on top of the pillar.

The CAM messages, like the others defined or under discussion in ETSI, are generated and elaborated at the facilities layer in order to provide relevant information to the applications. At the transmitting C-ITS-S, the messages generated at the facilities layer are passed down to the access layer, where the transmission over the wireless medium is performed. Then, the reversed path is followed at the destination.

To be remarked once more is that what hereafter detailed about aperiodic message generations with specific reference to CAMs, is expected to be valid for most of the messages currently under definition, including for example CPMs and VAMs.

A. CAM PACKET GENERATION

As defined in [22], CAMs are packets generated at the facilities layer and exchanged between C-ITS-Ss to be aware of each other and to support Day 1 applications. CAMs are estimated to represent in the early stage of deployment at least the 70% of the traffic load. These messages contain status and attribute information of the originating C-ITS-S. Specifically, in the case of vehicles, the status information includes time, position, motion state and activated systems, among others. The attribute information includes other data such as the dimensions, vehicle type and role in the road traffic. Some of the data elements of the CAM are mandatory, such as the station ID, timestamp, position, and status data (i.e., speed, heading, acceleration and curvature). Beside the mandatory information, the optional information may include, for example, the vehicle role or category, basic sensors, signatures and certificates.

The CAM generation is managed by the cooperative awareness basic service, which defines, in particular, the time interval between two consecutive CAM generations. To grant an efficient use of the spectrum and prevent congestion in the wireless channel, the actual generation time interval is in general variable and depends on the time-dependent behaviour of the C-ITS-S; for instance, changes in direction, position, speed, vehicle condition or the fact of being a special vehicle (e.g., an ambulance) influence the generation frequency. The upper and lower limits of the transmission interval are set to 0.1 s and 1 s, respectively, corresponding to an instantaneous CAM generation frequency between 10 Hz and 1 Hz. Within these limits, the CAM generation can be triggered according to the C-ITS-S dynamics and the channel congestion status. In case the dynamics of the originating C-ITS-S lead to a reduced CAM generation interval, this interval should be maintained for a number of consecutive CAMs.

More specifically, in terms of C-ITS-Ss dynamics, a new CAM generation is triggered when there is a direction change of the vehicle above 4° with respect to the previously transmitted message, or if the speed changed of more than 0.5 m/s, or finally, if the vehicle position changed of more than 4 m. Therefore, even when a vehicle is moving at constant speed and without changing its direction, the generation frequency depends on the vehicle speed. For example, the minimum packet generation periodicity (i.e., 1 Hz) corresponds to the vehicle moving at 14.4 km/h or below, while the maximum packet generation periodicity (i.e., 10 Hz) is obtained when the vehicle travels at a speed of 144 km/h or above. More in general, it was observed in [45] that the percentage of messages generated keeping the same generation interval as the previous one is only around 50%.

Assuming the generic vehicle moving at a constant speed, the generation interval, hereafter denoted as T_g, can be derived as a function of the speed. Specifically, denoting the speed as v in m/s, considering the minimum value $T_{g_{min}} = 100$ ms and the maximum value $T_{g_{max}} = 1$ s, and taking into

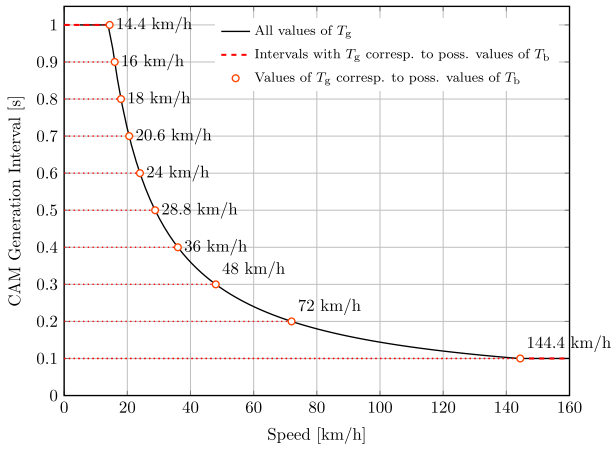

FIGURE 3. CAM generation period T_g as a function of the speed. The function is compared to the admissible values of the allocation period T_b.

account the triggering condition after 4 m, it is

$$T_g = \max\{\min\{4/v, T_{g_{max}}\}, T_{g_{min}}\} \quad (1)$$

which is shown in Fig. 3 (solid, black curve). As observable, the periodicity is larger at lower speed, where a less frequent update of the vehicle status is required, and smaller at higher speed, where the opposite is true. The behaviour of the curve shown in Fig. 3 is a consequence of the strictly linear increase in terms of generation frequency between its minimum and maximum values.

B. GENERATION AND ALLOCATION PERIOD

In the general case, the packet generation interval at the facilities layer T_g and the SB-SPS allocation period of LTE-V2X at the access layer T_b might differ from each other. In order to understand the implications of a mismatch between these two parameters, let us focus on the following two cases: i) when the allocation period is larger than the generation interval, i.e., $T_b > T_g$; and ii) when the allocation period is shorter than the generation interval, i.e., $T_b < T_g$.

Case when $T_b > T_g$: This case is illustrated in Fig. 4 assuming a periodic message generation: the higher part of the figure focuses on the messages generated at the facilities layer, with the messages indicated with capital letters from A to E; the lower part of the figure refers, instead, to the access layer, showing the resource grid and the allocation periodicity, and exemplifying the allocation and transmission processes for the messages received from the facilities layer. In the shown example, the subchannels allocated and used by packet A first and B later, are not suitable for the transmission of C, since it would imply a transmission delay which is larger than the maximum tolerated delay (corresponding to the LTE-V2X parameter T_2). Therefore, a reselection is triggered in LTE-V2X to reserve a new resource, which allows C to be transmitted within the window with extremes T_1 and T_2. This process is repeated also for the packet E. The reselection can be more or less frequent depending on the specific values of the generation and allocation periods.

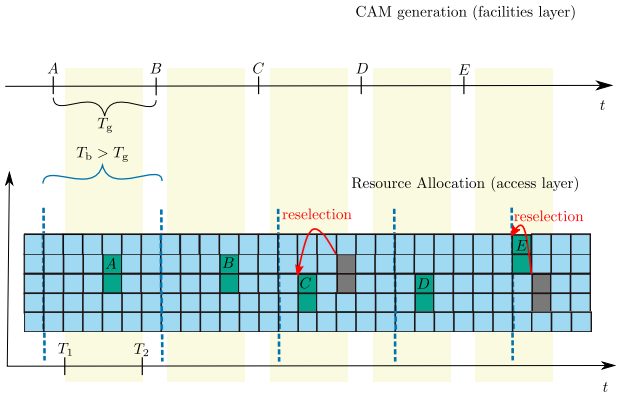

FIGURE 4. Example of CAM generation and allocation when $T_b > T_g$. The upper part illustrates the generation of five packets indicated with letters from *A* to *E*, and the selection window for each of these packets. The lower part illustrates the resource allocation process. The green squares represent the resources allocated for transmission. When the resource that was initially allocated is not within the selection window (see packets *C* and *E*) a reselection is required.

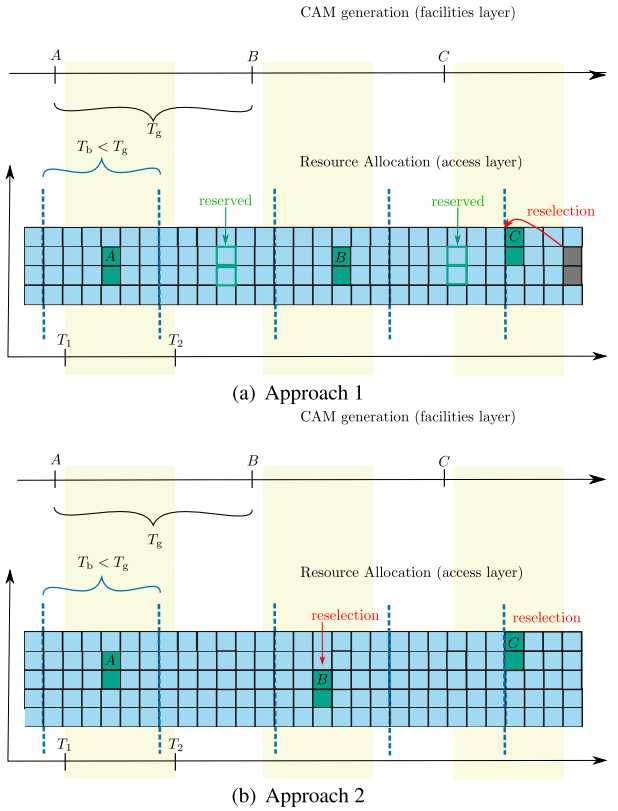

FIGURE 5. Example of CAM generation and allocation when $T_b < T_g$. The upper part illustrates the generation of five packets indicated with letters from *A* to *E*, and the selection window for each of these packets. The lower part illustrates the resource allocation. The green squares represent the resources allocated for transmission. When the resource that was initially allocated is not within the selection window (see packets *C* and *E*) a reselection is required.

Case when $T_b < T_g$: This case is illustrated in Fig. 5 assuming a periodic message generation. When the generation interval is large compared to the allocation period, it happens that no packets are present in the transmission

queue when the reserved resource is reached. How to deal with this situation in LTE-V2X does not appear defined in the specification and at least two options are possible:

- *Approach 1:* to maintain the resource allocation but leave the resource empty (exemplified in Fig. 5(a));
- *Approach 2:* to Release the resource and repeat the allocation process when the next message is received from the facilities layer (exemplified in Fig. 5(b)).

The two approaches are hereafter compared in terms of reselections and in Section V-C in terms of other performance metrics.[2] In the example of Fig. 5(a), Approach 1 is used: the resource previously allocated for the transmission of *A*, is left empty during the second allocation period because a new packet is not generated yet (see packet *B*). Although less frequent, a reselection can be anyway required also in this case (see packet *C*). Therefore, in Approach 1 the resource is maintained for multiple allocation periods according to the SB-SPS mechanism, while in Approach 2 the resource is maintained only for a single allocation period and then Released. In the example of Fig. 5(b), Approach 2 is used: the resource previously allocated for the transmission of *A*, is Released during the second allocation period because a new packet is not generated yet. When a new packet is generated (see packet *B*) a reselection is required.

In general, the less the two periods are aligned, the more the resources are allocated inefficiently. While the allocation period can take a few possible values (see Section III), the generation interval can be equal to any real number between 0.1 s and 1 s, depending on the vehicle dynamics. To remark this consideration, in Fig. 3 a vehicle is assumed to move at constant speed, and the corresponding T_g varying the vehicle speed is shown compared to the possible values of T_b between 100 ms and 1 s. Depending on the specific speed, which implies a given T_g, and the allocation period T_b, the situation can be the one described in Fig. 4 or the one in Fig. 5.

With the aim to determine the impact of this mismatch in terms of instability of the allocation process, we provide an analytical model for the average number of reselections per second, which depend on the setting of T_b, T_g, and T_2. An increase of the number of reselections indirectly causes a reduction of the system performance, since it reduces the effectiveness of the SB-SPS mechanism to individuate unused resources; this consideration is confirmed by the system simulations shown in Section V.

The proposed model neglects the number of allocations due to the SB-SPS algorithm, which are instead considered in the simulations used to validate such model. In particular, we consider the probability that a single packet is allocated and then the expected number of reselections per second is given by the number of packets per seconds multiplied by the probability of reselections per packet. Under the Approach 1, the expected number of reselections per seconds can be approximated as

$$\mathbb{E}\{n_r\} \simeq \max\left(\frac{1}{20\,T_b}, \min\left(\frac{P_r^{(1)}}{T_g} + \frac{P_r^{(1)}P_u^{(1)}}{2T_g}, \frac{1}{T_g}\right)\right) \quad (3)$$

where $P_r^{(1)}$ is defined in (2), with $m = \lfloor T_g/T_b \rfloor$, while $P_u^{(1)} = 1 - P_r^{(1)}$. Under the Approach 2, the expected number of reselections per seconds is

$$\mathbb{E}\{n_r\} \simeq \max\left(\frac{1}{20\,T_b}, \min\left(\frac{P_r^{(2)}}{T_g} + \frac{P_r^{(2)}P_u^{(2)}}{2T_g}, \frac{1}{T_g}\right)\right) \quad (4)$$

where $P_r^{(2)}$ is defined as

$$P_r^{(2)} = \begin{cases} 1 & T_g \le T_b - (T_2 - T_1) \\ \dfrac{T_b - T_g}{T_2 - T_1} & T_b - (T_2 - T_1) \le T_g \le T_b \\ \dfrac{T_g - T_b}{T_2 - T_1} & T_b \le T_g \le T_b + (T_2 - T_1) \\ 1 & T_g > T_b + (T_2 - T_1) \end{cases} \quad (5)$$

The derivation of (3) and (4) are given in the Appendix. The validity of the model is confirmed by the good agreement between analysis and simulations observable in Figs. 6 and 7.

Specifically, in Fig. 6 the average number of reselections per second performed by a vehicle moving at a constant speed is shown as a function of the speed, for $T_b \in \{0.1, 0.2, 0.3\}$. Both Approach 1 (maintain the resources) and Approach 2 (Release the resources) are considered for the situation where $T_b < T_g$. $T_1 = 0$ s and $T_2 = 0.1$ s is assumed.

Focusing on Approach 1, when $T_b = 0.1$ s, we see that the number of reselections remains always constant at 0.5. Note that in this case the generation interval is greater or equal to the allocation period for any speed value (see Fig. 3) and that

[2]Focusing on Approach 2, two variants have been considered: the first one, denoted *conventional*, where neither SCI or TB are transmitted; the second one, denoted *SCI with empty TB*, where the SCI is transmitted, even if there is no data to transmit; the aim of the latter variant is to let the neighboring vehicles know that the resource is reserved. However, given that the allocation procedure mostly relies on the average measured power, the performance observed with the two approached was almost identical. For this reason, in this paper results are reported only adopting the *conventional* case.

$$P_r^{(1)} = \begin{cases} \dfrac{T_b - (T_2 - T_1)}{T_2 - T_1} & (m+1)T_b - (T_2 - T_1) < T_g \le mT_b + (T_2 - T_1) \\ \dfrac{T_g - mT_b}{T_2 - T_1} & T_g \le mT_b + (T_2 - T_1),\ T_g \le (m+1)T_b - (T_2 - T_1) \\ \dfrac{(m+1)T_b - T_g}{T_2 - T_1} & T_g > mT_b + (T_2 - T_1),\ T_g > (m+1)T_b - (T_2 - T_1) \\ 1 & mT_b + (T_2 - T_1) < T_g \le (m+1)T_b - (T_2 - T_1) \end{cases} \quad (2)$$

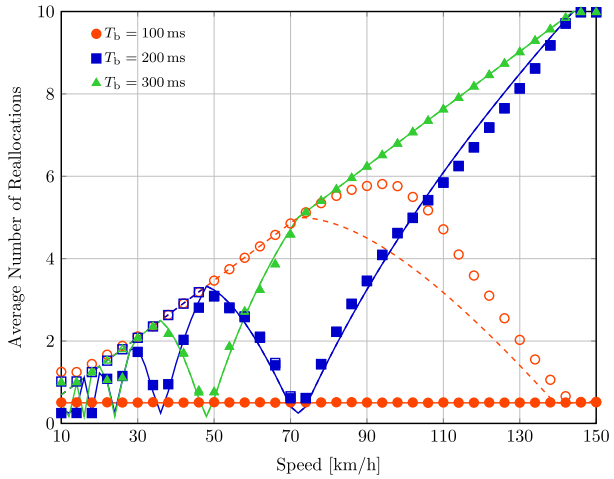

FIGURE 6. Average number of reselections per second per vehicle as a function of the vehicle speed and for different duration of the allocation period T_b, assuming the maximum latency $T_2 = 100$ ms. Solid lines are obtained with Approach 1. Dashed lines are obtained with Approach 2 (analytical model). Full markers are obtained with Approach 1 (simulation). Empty markers are obtained with Approach 2 (simulation).

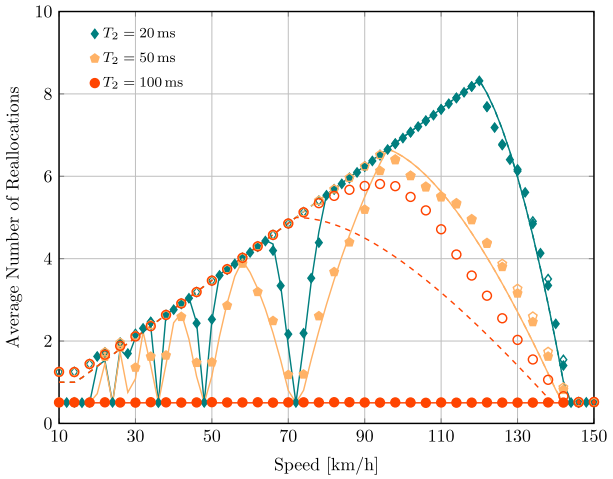

FIGURE 7. Average number of reselections per second per vehicle, as a function of the vehicle speed and for different duration of the maximum latency parameter T_2, assuming the duration of the allocation period $T_b = 0.1$ ms. Solid lines are obtained with Approach 1 (analytical model). Dashed lines are obtained with Approach 2 (analytical model). Full markers are obtained with Approach 1 (simulation). Empty markers are obtained with Approach 2 (simulation).

$T_b = T_2$. With $T_b = 0.2$ s, the generation interval is lower than the allocation period for any speed greater than 72 km/h (refer to Fig. 3). When the speed is exactly 72 km/h, $T_b = T_g$ and Fig. 6 shows a local minimum. The same curve has a local minimum also at 38 km/h, which corresponds to a generation interval equal to 0.4 s (see Fig. 3), i.e., a multiple of T_b. Indeed, a local minimum is expected for every value of the generation interval that is equal or multiple of the allocation period. For $T_b = 0.3$ s, the generation interval is below the allocation period for speed values greater than 48 km/h (see Fig. 3). Interestingly, for the same speed value Fig. 6 shows a minimum equal to 0.17, which is lower than that obtained assuming $T_b = 0.2$ s, i.e. 3.31. The same minimum is again achieved when T_g is another multiple of T_b. For any speed except around the local minima, the lowest $T_b = 0.1$ s allows the minimum average number of reselections. Focusing on Approach 2, the average number of reselections is always higher or equal to the one of Approach 1. In particular, for any value of T_b, the average number of reselections increases linearly for lower values of the speed, and then decreases in alignment with the case of Approach 1. In particular, the linear increase is maintained up to 36 km/h and 48 km/h for $T_b = 0.3$ s and $T_b = 0.2$ s, respectively.

Similar results are shown in Fig. 7 assuming $T_b = 0.1$ s and varying the maximum latency given by T_2. Recall that T_2 is a parameter that can be set in LTE-V2X for QoS configuration. The figure shows that such maximum latency impacts remarkably on the number of required reselections. Indeed, the number of reselections for the case $T_b = 0.1$ s in Fig. 6 was approximately constant for $T_2 = 0.1$ s; differently, when the maximum latency decreases, the number of reselections increases remarkably. Also in this case and for both $T_2 = 20$ ms and $T_2 = 50$ ms, there are local minima for the speed values corresponding to a generation interval equal or multiple of the allocation period. Indeed, as observable in Fig. 3, multiples of 0.1 s are for example obtained with speed equal to 36 km/h, corresponding to $T_g = 0.4$, with speed equal to 48 km/h, corresponding to $T_g = 0.3$, and with speed equal to 72 km/h, corresponding to $T_g = 0.2$.

V. SYSTEM LEVEL RESULTS FROM THE CASE STUDY

In this section, we present system level simulation results for a case study in a highway scenario, adopting the open source LTEV2Vsim simulator [46].[3] An insight on simulation settings and performance metrics is provided before discussing numerical results.

A. SIMULATION SETTINGS

In this subsection, the settings of the simulations are detailed in terms of scenario, propagation and packet loss modeling, facilities layer, and access layer. A summary is also provided in Table 1.

1) SCENARIO

We assume 50 or 100 vehicles/km moving on a 3 + 3 lanes and or 200 vehicles/km moving on a 6+6 lanes, considering a 2 km long straight highway with wrap-around (i.e., a vehicle exiting on one side of the scenario, enters from the other side in the same lane).

In order to better focus on the considerations subject of this research, the average speed of the vehicles is set to a specific value, assumed between 10 km/h and 150 km/h, in steps of 2 km/h. Each vehicle moves at a randomly selected speed with Gaussian distribution around the given average, with a

[3]LTEV2Vsim is an open source simulator, available at https://github.com/alessandrobazzi/LTEV2Vsim

TABLE 1. Main simulation parameters and settings.

Scenario	
Road layout	Highway, 3+3 or 6+6 lanes
Density	50, 100, 200 vehicles/km
Speed	Variable
Power and propagation	
Channels	ITS bands at 5.9 GHz
Bandwidth	10 MHz
Transmission power density	13 dBm/MHz
Antenna gain (tx and rx)	3 dBi
Noise figure	6 dB
Propagation model	WINNER+, Scenario B1
Shadowing	Variance 3 dB, decorr. dist. 25 m
Fast fading	Highway LOS fading model
Facilities layer (LTE-V2X)	
Beacon periodicity	Derived from speed
Beacon size	350 byte
Access layer (LTE-V2X)	
MCS	7 (QPSK, ∼0.58) PER=0.1@SINR=4.1dB
Subchannel size	10 physical resource block pairs (3 subchannels per packet)
SCI Configuration	Adjacent
Keep probability	0.5
Subchannel sensing threshold	-110 dBm
Min. time for the allocation, T_1	0
Max. time for the allocation, T_2	20, 50, 100 ms

standard deviation always equal to one-tenth of the average speed.

2) POWER SETTINGS, PROPAGATION, AND LOSS MODELING

The devices transmit in one 10 MHz large channel of the 5.9 GHz band (the specific channel that is used appears irrelevant to the scope of the paper), with a constant spectral power density of 13 dBm/MHz[4] and have an antenna gain at both the transmitter and receiver equal to 3 dBi.[5] The noise figure of the receiver is assumed equal to 6 dB.[6] For the path-loss, the WINNER+, scenario B1, with correlated log-normally distributed shadowing, characterized by a standard deviation of 3 dB and a decorrelation distance of 25 m is used, as in [1]. Given the highway scenario, line-of-sight (LOS) conditions are assumed. For each potentially received packet, the average signal-to-interference-plus-noise ratio (SINR) is calculated by taking into account the interference from all the other nodes. Once the SINR is calculated, the correct reception of each packet is statistically drawn from packet error rate (PER) vs. SINR curves, derived via link level simulations which take into account the impact of small-scale fading. In this work, the curves detailed in [47] are used, obtained assuming 1 transmitting antenna and 2 receiving antennas with 1×2 IRC (Hermitian noise covariance Matrix) equalizer, highway LOS fading model as per [48], channel estimate based on preamble and feedback loop, perfect control channel decoding, and perfect synchronization.

3) SETTINGS AT THE FACILITIES AND ACCESS LAYERS

At the facilities layer, messages of 350 bytes are supposed, which is the size of CAMs occurring with highest probability in [45]. Even if the size of CAMs is in general variable, as shown for example in [21], a fixed size is here assumed to focus the attention on the generation interval.

At the access layer, 5 subchannels of 10 physical resource block pairs (PRBPs) each are used as mandate by [49]. Additionally, the MCS 7 is used, which corresponds to QPSK modulation and 3 subchannels required to transmit a 350 bytes packet.

B. PERFORMANCE METRICS

We present simulation results based on the packet reception ratio (PRR), which is the average ratio between the number of neighbours correctly decoding a CAM at a given distance and the total number of neighbours at the same distance.

Specifically, we will consider the range with PRR > 0.9 and the value of PRR at a reference distance of 100 m.

C. RESULTS COMPARING DIFFERENT APPROACHES WHEN RESERVED RESOURCE IS REACHED WITH EMPTY QUEUE

In this subsection, results with $T_2 = 0.1$ s and variable T_b are shown for the two approaches, namely Approach 1 and Approach 2, proposed for the handling of reserved resources with empty queue (see Section IV-B). Results are obtained with a density equal to 50 vehicles/km.

Fig. 8(a) shows the range with PRR greater than 0.9 vs. the average speed for Approach 1, varying the allocation period T_b. The figure shows that such a metric, which could be expected to decrease with the generation interval (implicitly decreasing when the average speed increases), actually follows a trend that is coherent with the variation of the number of reselections. Specifically, for $T_b = 0.1$ s, the range with PRR > 0.9 is monotonically and slowly decreasing. Recall that in this case the number of reselections is constant as the speed varies (see Fig. 6). For $T_b = 0.2$ s, the range with PRR > 0.9 is not monotonically decreasing with the speed and local maxima are found at 24 km/h (corresponding to $T_g = 3 \cdot T_b$), 36 km/h (corresponding to $T_g = 2 \cdot T_b$) and 72 km/h (corresponding to $T_g = T_b$), where the range with PRR > 0.9 is 340 m, 340 m, and 330 m, respectively. Finally, for $T_b = 0.3$ s, the range with PRR > 0.9 is also not monotonically decreasing with the speed and two local maxima are found at 24 km/h and 48 km/h, where the range with PRR $>$ 0.9 is 340 m. In general, the value $T_b = 0.1$ s looks always preferable for the speed values considered. Fig. 8(b) shows the range with PRR greater than 0.9 for Approach 2 and varying the allocation period. The metric is monotonically decreasing in this case, coherently with the variation of the number of reselections (i.e., monotonically increasing). For any value of T_b, and for any speed, the performance is

[4]A spectral power density of 13 dBm/MHz corresponds to 23 dBm if the full 10 MHz channel is used, which a common value for commercial devices.

[5]An antenna gain of 3 dBi appears as a realistic average value over the Azimuth plane. An example antenna is the MobileMark SMW314.

[6]A noise figure of 6 dB is for example indicated for the NXP RoadLINK SAF5400 modem.

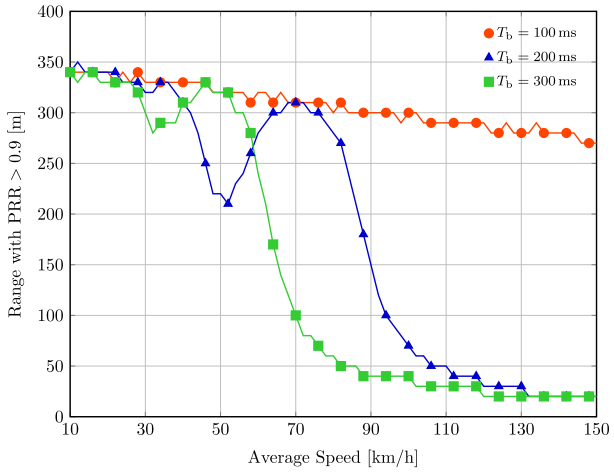

(a) Approach 1

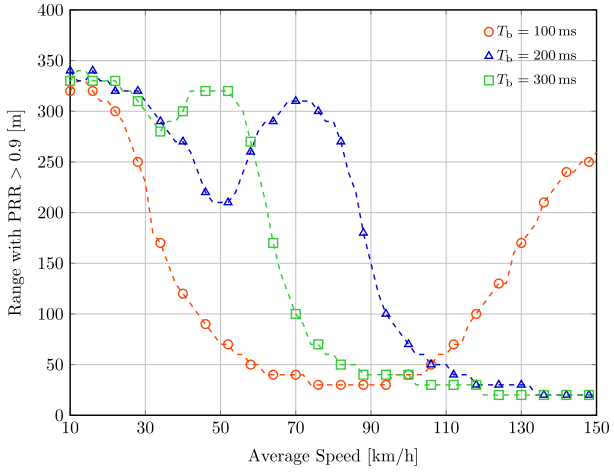

(b) Approach 2

FIGURE 8. Range with PRR greater than 0.9 is shown as a function of the vehicle speed and varying the allocation period duration, with 50 vehicles/km, and considering two approaches for handling the reserved resources with an empty queue.

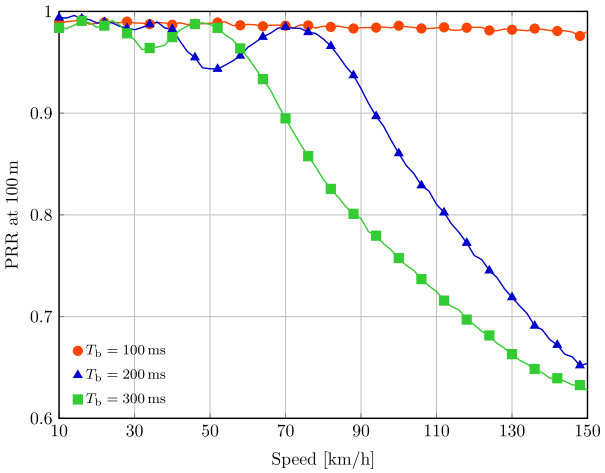

(a) Approach 1

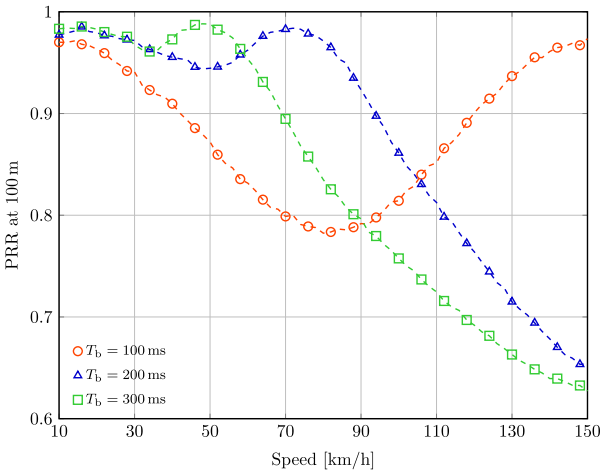

(b) Approach 2

FIGURE 9. PRR measured at 100 meters, as a function of the vehicle speed and varying the allocation period duration. Results are obtained with density equal to 50 vehicles/km.

remarkably worse than the one obtained with Approach 1, confirming that frequent reselections have a significantly negative impact on the ability on LTE-V2X reliability, due to the inaccuracy that this causes in the estimation of available CSSRs.

Same conditions, but with a different point of view, are considered in Fig. 9(a) and Fig. 9(b), where the PRR obtained at 100 m is shown varying the average speeed with Approach 1 and 2, respectively. Focusing on Approach 1, this metric shows the same trend as the range with PRR $>$ 0.9. Specifically, when $T_b = 0.1$ s, the PRR at 100 m is 0.99 at 10 km/h and decreases monotonically and slowly up to 0.98 for 150 km/h. When $T_b = 0.2$ s, the PRR at 100 m shows local maxima, equal to 0.99 at 36 km/h and 72 km/h and then decreases monotonically and fast up to 0.65 at 150 km/h. When $T_b = 0.3$ s in the scenario with 100 vehicles, the PRR at 100 m shows two local maxima, equal to 0.99 at 24 km/h and 48 km/h and then decreases monotonically and fast up to 0.63 at 150 km/h.

As an overall remark following the shown results, Approach 1, i.e., maintaining the resource allocation although leaving the resource empty, appears clearly the best approach. Therefore, in the rest of this Section, we will focus only on Approach 1. Focusing on this approach, it can be also concluded that under non-congested channel conditions and given $T_2 = 0.1$ s, the use of $T_b = 0.1$ s always allows better performance than larger T_b. More congested conditions and smaller values for T_2 are considered in the following subsections.

D. RESULTS VARYING THE VEHICLE DENSITY

In this subsection, we show the same performance metrics as in Section V-C, focusing on Approach 1, while considering two larger values for the vehicle density: 100 and 200 vehicles/km. Results are obtained with a maximum latency $T_2 = 0.1$ s, and varying the allocation period.

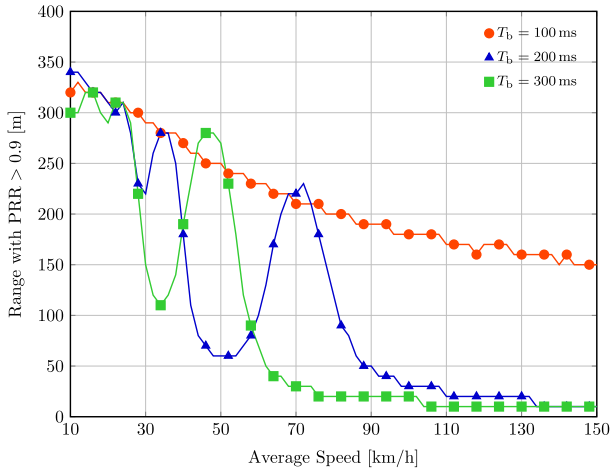

(a) 100 vehicles/km

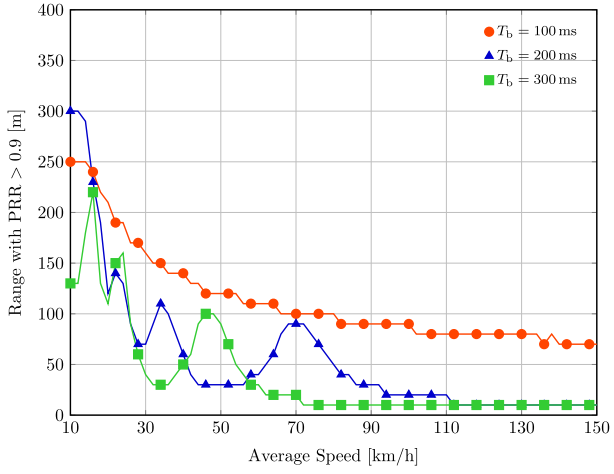

(b) 200 vehicles/km

FIGURE 10. Range with PRR > 0.9 where a PRR greater than 0.9 is obtained, as a function of the vehicle speed and varying the allocation period duration. Results are obtained with density equal to 100 and 200 vehicles/km.

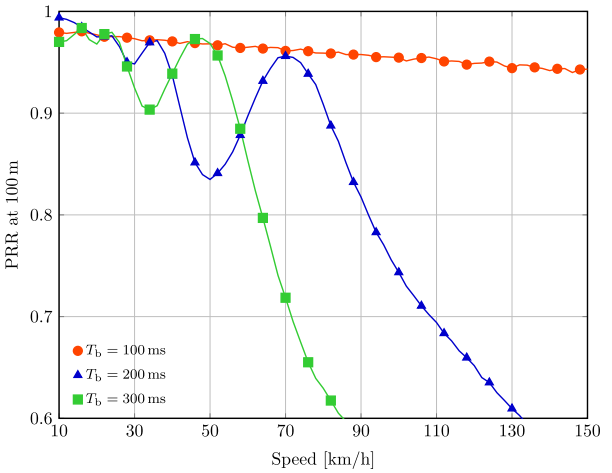

(a) 100 vehicles/km

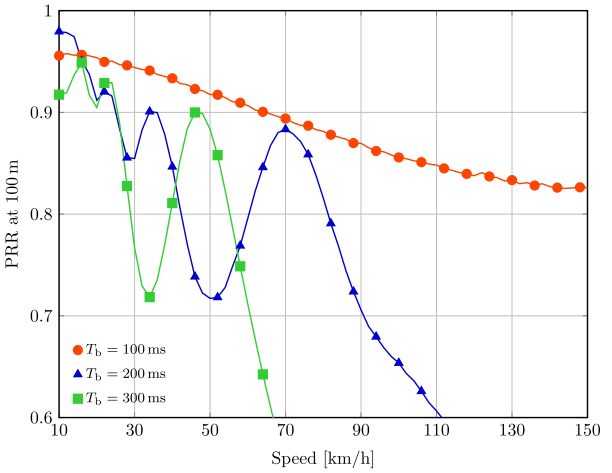

(b) 200 vehicles/km

FIGURE 11. PRR measured at 100 meters, as a function of the vehicle speed and varying the allocation period duration. Results are obtained with density equal to 100 and 200 vehicles/km.

Figures 10(a) and 10(b) show the range with PRR $>$ 0.9 assuming 100 and 200 vehicles/km, respectively. The figure shows that the trend followed by the range with PRR $>$ 0.9 as a function of the speed is in line with Fig. 8(a) and that an increase of the vehicle density worsens the performance, i.e. the metric decreases faster. For example, when T_b = 0.1 and 100 vehicles/km, the range is 320 m at 10 km/h and 150 m at 150 km/h, respectively compared to 340 m and 280 m obtained with 50 vehicles/km. With 200 vehicles/km, range with PRR $>$ 0.9 further worsens to 250 m at 10 km/h and 70 m at 150 km/h. It can also be noted that with the higher density, in a few very specific cases, adopting other values of T_b than 0.1 s is the optimal choice. As specific examples, this occurs with an average speed between 70 and 72 km/h adopting $T_b = 0.2$ and with an average speed between 44 and 50 km/h adopting $T_b = 0.3$. In these specific cases, the generation period T_g is compliant with the allocation period T_b, thus the reselections do not increase relevantly and a larger allocation period T_b allows to maintain the same allocation for a time which is on average longer.[7] The improvement compared to $T_b = 0.1$ s is anyway small and the use of the latter seems a reasonable solution in all cases.

Fig. 11(a) and Fig. 11(b) show the PRR at 100 m under the same conditions, i.e., assuming 100 and 200 vehicles/km, respectively, with different values of T_b. In the scenario with 100 vehicles/km, the performance are worsened by the higher density and the decrease of the PRR is faster with the speed. Nevertheless, the trends remain the same. For example, when $T_b = 0.2$ s, the PRR decreases non-monotonically from 0.99 at 10 km/h to 0.55 at 150 km/h. The two local maxima are at 34 km/h and 70 km/h. The effect of misalignment is very evident for a speed value of 50 km/h, where we have a lower

[7]With the allocation period $T_b > 0.1$ s, the SB-SPS algorithm foresees that the same CSSR is maintained for a number of periods uniformly randomly selected between 5 and 15, then confirmed or changed based on the keep probability p_k. Assuming $p_k = 0.5$, this means that the same CSSR is kept on average for $20 \cdot T_b$ s, which is proportional to T_b.

PRR with $T_b = 0.2$ s, i.e. 0.83, than with $T_b = 0.3$ s, i.e. 0.97. A further increase of the density, i.e. with 200 vehicles/km, leads to the same conclusion. Indeed, for a speed value of 50 km/h, where the PRR with $T_b = 0.2$ s is 0.83 and with $T_b = 0.3$ s is 0.97. The use of $T_b = 0.1$ s appears thus preferable from the point of view of this metric in both scenarios and for almost all the values of the average speed.

Overall, it is noted that, even if the value of T_b allowing the highest PRR depends on the specific conditions, the use of $T_b = 0.1$ s appears optimal in most of the cases and near to optimal in the few remaining, for any average speed (and the consequent generation period T_g) and density. It is to note that $T_b = 0.1$ s is the minimum value that can be used with the maximum delay T_2 set to 0.1 s.

E. RESULTS VARYING THE MAXIMUM TRANSMISSION DELAY

In this subsection, we investigate the relationship between T_g and T_b assuming a smaller value of the maximum delay $T_2 =$ 20 ms. Results are obtained with 50 vehicles/km.

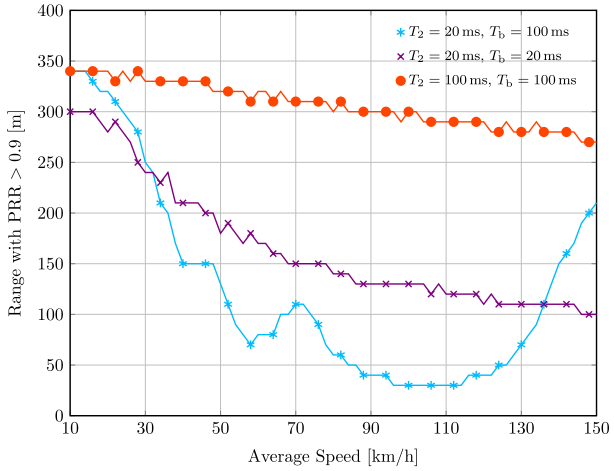

FIGURE 12. Range with PRR > 0.9 where a PRR greater than 0.9 is obtained, as a function of the vehicle speed and varying the allocation period duration and the maximum time for the allocation. Results are obtained with 50 vehicles/km.

Fig. 12 shows the range with PRR > 0.9 assuming the combinations of $T_b = 20$ ms and 100 ms, as well as $T_2 = 20$ ms and 100 ms. Under the same conditions, Fig. 13 presents the PRR at 100 m. To note that $T_b = 20$ ms constraints the delay to 20 ms and thus the case $T_b = 20$ ms and $T_2 = 100$ ms is not considered.

Focusing on the cases with $T_2 = 20$ ms, Figs. 12 and 13 show that the use of the smaller $T_b = 20$ ms is preferable at medium and medium-high speeds (between 30 and 130 km/h). For example, when the speed is 70 km/h, the range with PRR > 0.9 is 150 m for $T_b = 20$ ms and $T_2 = 20$ ms, whereas it is reduced to 110 m for $T_b = 100$ ms and $T_2 = 20$ ms. The conclusion is in line with what observed assuming $T_2 = 100$ ms, suggesting that the use of the smallest periodicity among those compliant with T_2 can be a good

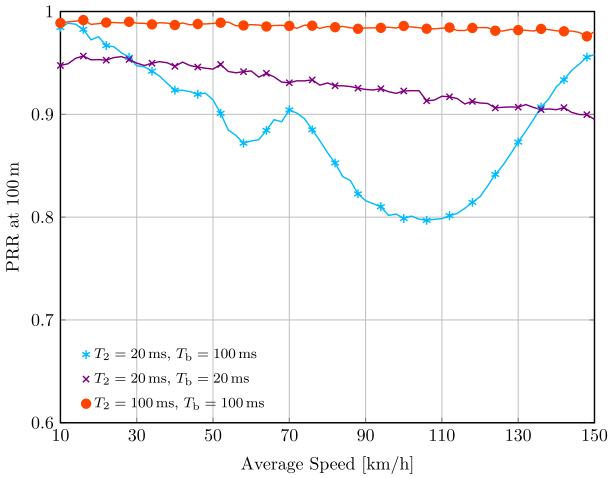

FIGURE 13. PRR measured at 100 meters, as a function of the vehicle speed and varying the allocation period duration and the maximum time for the allocation. Results are obtained with 50 vehicles/km.

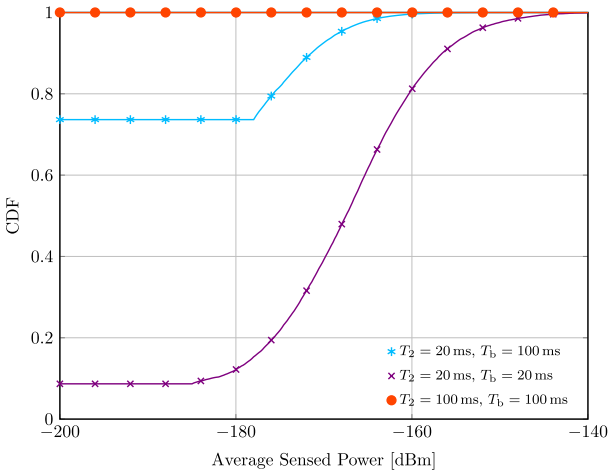

FIGURE 14. CDF of the sensed power averaged over the selected subset of resources, varying the allocation period duration and the maximum time for the allocation. Results are obtained with 50 vehicles/km and speed of 50 km/h.

solution in general. The point is that a lower T_b implies overall less reselections. Exceptions are however observable when T_g is exactly a multiple of T_b for the majority of vehicles, i.e., when $T_b = 1$ s and the average speed is below 14 km/h or $T_b = 100$ ms and the average speed is above 144 km/h. In such cases, as explained hereafter commenting Fig. 14, a better individuation of the free CCSR is allowed by the larger T_b. The performance trend is confirmed by Fig. 13 showing the PRR at 100 m.

As already anticipated, the conclusion is not that the choice of the shortest T_b is in general the best solution. This can be further observed nothing that the case with $T_b = 100$ ms and $T_2 = 100$ ms is also considered, it is noted that it always outperforms the case with $T_b = 20$ ms (and $T_2 = 20$ ms). Please remark that this does not occur due to less time-frequency resources overall used, since instead

the number of transmitted messages remains the same. The motivation is rather that a longer T_b allows for a larger number of CSSRs and thus higher effectiveness of the SB-SPS. This consideration is further explained through Fig. 14, where the cumulative distribution function (CDF) of the sensed power averaged over the sensing period is shown for the selected subset of the CSSRs. With selected subset of CSSRs we mean the 20% of the available CSSRs, obtained based on both received power and information retrieved from the received SCIs, among which the next CSSRs to be used is randomly selected. As visible in Fig. 14, when $T_2 = 100$ ms, the power level is much higher for the case $T_b = 20$ ms than the case $T_b = 100$ ms. In particular, with $T_b = T_2 = 100$ ms the average sensed power is always below -200 dB, meaning that none of the selected resources are used by neighboring nodes. With $T_b = 100$ ms and $T_2 = 20$ ms, the total number of CSSRs is the same, but the selected ones are taken only from the first 20 ms, reducing the probability to have an average sensed power below -200 dBm to 0.74. When $T_b = T_2 = 20$ ms, the entire pool of CSSRs is reduced to one fifth compared to $T_b = 100$ ms and looking at the selected 20% the probability to have an average sensed power below -200 dBm falls to 0.09, which means that a non-interfered resource is chosen only in the 9% of cases.

Summarizing the results provided through Figs. 12-14, it can be concluded that: (i) given a certain T_2, the smallest T_b is always preferable when T_g cannot be a multiple of T_b, which is coherent with what concluded in Section V-D; (ii) that a larger T_b is preferable only if T_g is a multiple of such value; and (iii) that the use of a smaller T_2 causes a performance loss, implying a trade-off between latency and reliability.

VI. CONCLUSION

In this work, the effect of a mismatch between the packet generation at higher layers and the periodical structure of resources at the lower layers of sidelink C-V2X autonomous mode is investigated. The study is done focusing on LTE-V2X and CAM generation, but it is expected to provide general conclusions valid also for 5G-V2X and for most of the other messages currently under definition. Results have shown that performance reduces as soon as the packet is not generated using the same periodicity as the allocation process, although they appear always near to optimal if resources are reserved more frequently than needed, simply leaving them unused when the transmission buffer is empty. At the same time, it is also noted that the reduction of the maximum delay, which is a parameter left for optimization, has a negative impact on the reliability; thus, the maximum delay should be relaxed as much as allowed by the application, and then the allocation periodicity should be reduced to the minimum value compatible with such constrain. It follows that if the delay constraint can be set to 100 ms (i.e. the maximum allowed), a practical solution is to set the allocation period to 100 ms. Overall, it has been shown that the considered mismatch, expected to be common in real implementations, has a possible detrimental effect on the performance of the system and thus require careful setting of the parameters and appropriate definition of those procedures that are not specified.

APPENDIX
ANALYTICAL MODEL

In this appendix, the analytical model for the average number of reselections is derived. Without loss of generality, let us consider that a reselection has been made for a packet arriving at t_g, and therefore, the resource is allocated at t_b that is uniformly distributed in $[t_g + T_1, t_g + T_2]$.

A. APPROACH 1

Under Approach 1, the next packet is generated at $t_g + T_g$, which falls within the allocation period $[mT_b, (m+1)T_b)$, where $m = \lfloor T_g/T_b \rfloor$. Within such an allocation period, the next resource is allocated at $(m+1)T_b + t_b$. Then, a new reselection is required if the resource is allocated after the maximum delay is expired and belongs to the subsequent allocation period, i.e.

$$\mathcal{R} = \left\{ \begin{matrix} mT_b + t_b < t_g + T_g \\ (m+1)T_b + t_b > t_g + T_g + (T_2 - T_1) \end{matrix} \right\} . \quad (6)$$

Then the probability of reselection for a single packet generation is

$$P_r^{(1)} = \int_{\max(T_2-T_1, T_g - mT_b)}^{\min(T_2-T_1, T_g-mT_b)} 1/(T_2 - T_1)\, dt_b . \quad (7)$$

The expected value for the number of reselections per second n_r, should be calculated also considering the probability that the resource is not reallocated but used for the packet at T_g, i.e. $P_u = 1 - P_r$. In case the resource is used, a new reselection can be required for the following packet, in which case the time between two consecutive reselections would be $2\,T_g$. We then approximate the average number of reselections as

$$\mathbb{E}\{n_r\} \simeq \frac{1}{T_g} P_r^{(1)} + \frac{1}{2T_g} P_u P_r^{(1)} . \quad (8)$$

where we are neglecting all the terms after the second packet (i.e., when no reselection is required for the packet at $2T_g$). The solution of the integral in (7) leads to the equation (3).

B. APPROACH 2

Under Approach 2, the next packet is generated at $t_g + T_g$. A reselection is always required unless $t_b + T_b > t_g + T_g$. In this case, the allocation is also required if $t_b + T_b > t_g + T_g + T_2$. Then the probability of reselection for a single packet generation is

$$P_r^{(2)} = \int_{\max(T_2-T_1, T_g+T_2-T_b)}^{\min(T_2-T_1, T_g-T_b)} 1/(T_2 - T_1)\, dt_b . \quad (9)$$

The expected value for the number of reselections per second n_r is analogous to (8). The solution of the integral in (9) leads to the equation (4).

REFERENCES

[1] *Technical Specification Group Radio Access Network; Study on LTE-Based V2X Services*, Standard 3GPP TR 36.885 v16.2.0, Jul. 2019.

[2] *Vehicle to Vehicle (V2V) Services Based on LTE Sidelink; User Equipment (UE) Radio Transmission and Reception; Release 14*, Standard 3GPP TR 36.785 v14.0.0, Oct. 2016.

[3] *Study on LTE Support for Vehicle to Everything (V2X) Services; RElease 14*, Standard 3GPP TR 22.885 v16.2.0, Dec. 2015.

[4] *Study on Architecture Enhancements for LTE Support of V2X Services; Release 14*, Standard 3GPP TR 23.785 v14.0.0, Sep. 2016.

[5] M. Gonzalez-Martin, M. Sepulcre, R. Molina-Masegosa, and J. Gozalvez, "Analytical models of the performance of C-V2X mode 4 vehicular communications," *IEEE Trans. Veh. Technol.*, vol. 68, no. 2, pp. 1155–1166, Feb. 2019.

[6] *Technical Specification Evolved Universal Terrestrial Radio Access (E-UTRA); Radio Resource Control (RRC); Protocol Specification; Release 16*, Standard 3GPP TS 36.331 v16.2.1, 2016.

[7] S. Chen, J. Hu, Y. Shi, Y. Peng, J. Fang, R. Zhao, and L. Zhao, "Vehicle-to-everything (v2x) services supported by LTE-based systems and 5G," *IEEE Commun. Standards Mag.*, vol. 1, no. 2, pp. 70–76, Jul. 2017.

[8] G. Naik, B. Choudhury, and J.-M. Park, "IEEE 802.11bd & 5G NR V2X: Evolution of radio access technologies for V2X communications," *IEEE Access*, vol. 7, pp. 70169–70184, 2019.

[9] W. Anwar, N. Franchi, and G. Fettweis, "Physical layer evaluation of V2X communications technologies: 5G NR-V2X, LTE-V2X, IEEE 802.11bd, and IEEE 802.11p," in *Proc. IEEE 90th Veh. Technol. Conf. (VTC-Fall)*, Sep. 2019, pp. 1–7.

[10] C. Campolo, A. Molinaro, F. Romeo, A. Bazzi, and A. O. Berthet, "5G NR V2X: On the impact of a flexible numerology on the autonomous sidelink mode," in *Proc. IEEE 2nd 5G World Forum (5GWF)*, Sep. 2019, pp. 102–107.

[11] B. Ji, X. Zhang, S. Mumtaz, C. Han, C. Li, H. Wen, and D. Wang, "Survey on the Internet of vehicles: Network architectures and applications," *IEEE Commun. Standards Mag.*, vol. 4, no. 1, pp. 34–41, Mar. 2020.

[12] B. Ji, Y. Han, P. Li, S. Mumtaz, K. Song, C. Li, D. Wang, and H. Wen, "Research on secure transmission performance of electric vehicles under Nakagami-m channel," *IEEE Trans. Intell. Transp. Syst.*, early access, Nov. 3, 2020, doi: 10.1109/TITS.2020.3030540.

[13] H. Liang, J. Wu, S. Mumtaz, J. Li, X. Lin, and M. Wen, "MBID: Micro-blockchain-based geographical dynamic intrusion detection for V2X," *IEEE Commun. Mag.*, vol. 57, no. 10, pp. 77–83, Oct. 2019.

[14] V. Sharma, I. You, and N. Guizani, "Security of 5G-V2X: Technologies, standardization, and research directions," *IEEE Netw.*, vol. 34, no. 5, pp. 306–314, Sep. 2020.

[15] R. Lu, L. Zhang, J. Ni, and Y. Fang, "5G vehicle-to-everything services: Gearing up for security and privacy," *Proc. IEEE*, vol. 108, no. 2, pp. 373–389, Feb. 2020.

[16] S.-Y. Lien, D.-J. Deng, C.-C. Lin, H.-L. Tsai, T. Chen, C. Guo, and S.-M. Cheng, "3GPP NR sidelink transmissions toward 5G V2X," *IEEE Access*, vol. 8, pp. 35368–35382, 2020.

[17] F. Abbas, P. Fan, and Z. Khan, "A novel low-latency V2 V resource allocation scheme based on cellular V2X communications," *IEEE Trans. Intell. Transp. Syst.*, vol. 20, no. 6, pp. 2185–2197, Jun. 2019.

[18] Q. Chen, H. Jiang, and G. Yu, "Service oriented resource management in spatial reuse-based C-V2X networks," *IEEE Wireless Commun. Lett.*, vol. 9, no. 1, pp. 91–94, Jan. 2020.

[19] R. Aslani, E. Saberinia, and M. Rasti, "Resource allocation for cellular V2X networks mode-3 with underlay approach in LTE-V standard," *IEEE Trans. Veh. Technol.*, vol. 69, no. 8, pp. 8601–8612, Aug. 2020.

[20] A. Bazzi, G. Cecchini, A. Zanella, and B. M. Masini, "Study of the impact of PHY and MAC parameters in 3GPP C-V2 V mode 4," *IEEE Access*, vol. 6, pp. 71685–71698, 2018.

[21] R. Molina-Masegosa, M. Sepulcre, J. Gozalvez, F. Berens, and V. Martinez, "Empirical models for the realistic generation of cooperative awareness messages in vehicular networks," *IEEE Trans. Veh. Technol.*, vol. 69, no. 5, pp. 5713–5717, May 2020.

[22] *Intelligent Transport Systems (ITS); Vehicular Communications; Basic Set of Applications; Part 2: Specification of Cooperative Awareness Basic Service*, Standard 3GPP EN 302.637-2 v1.3.1 Sep. 2014.

[23] R. Molina-Masegosa and J. Gozalvez, "LTE-V for sidelink 5G V2X vehicular communications: A new 5G technology for short-range vehicle-to-everything communications," *IEEE Veh. Technol. Mag.*, vol. 12, no. 4, pp. 30–39, Dec. 2017.

[24] J. Hu, S. Chen, L. Zhao, Y. Li, J. Fang, B. Li, and Y. Shi, "Link level performance comparison between LTE V2X and DSRC," *J. Commun. Inf. Netw.*, vol. 2, no. 2, pp. 101–112, Jun. 2017.

[25] V. Mannoni, V. Berg, S. Sesia, and E. Perraud, "A comparison of the V2X communication systems: ITS-G5 and C-V2X," in *Proc. IEEE 89th Veh. Technol. Conf. (VTC-Spring)*, Apr. 2019, pp. 1–5.

[26] J. Thota, N. F. Abdullah, A. Doufexi, and S. Armour, "V2V for vehicular safety applications," *IEEE Trans. Intell. Transp. Syst.*, vol. 21, no. 6, pp. 2571–2585, Jun. 2019.

[27] J. Kim, O. Jo, and S. W. Choi, "Feasibility of index-coded retransmissions for enhancing sidelink channel efficiency of V2X communications," *IEEE Access*, vol. 7, pp. 6545–6552, 2019.

[28] L. F. Abanto-Leon, A. Koppelaar, and S. H. de Groot, "Enhanced C-V2X mode-4 subchannel selection," in *Proc. IEEE 88th Veh. Technol. Conf. (VTC-Fall)*, Aug. 2018, pp. 1–5.

[29] A. Masmoudi, S. Feki, K. Mnif, and F. Zarai, "Efficient scheduling and resource allocation for D2D-based LTE-V2X communications," in *Proc. 15th Int. Wireless Commun. Mobile Comput. Conf. (IWCMC)*, Jun. 2019, pp. 496–501.

[30] H. D. R. Albonda and J. Perez-Romero, "An efficient mode selection for improving resource utilization in sidelink V2X cellular networks," in *Proc. IEEE 23rd Int. Workshop Comput. Aided Modeling Design Commun. Links Netw. (CAMAD)*, Sep. 2018, pp. 1–6.

[31] P. Wendland, G. Schaefer, and R. S. Thoma, "LTE-V2X mode 4: Increasing robustness and DCC compatibility with reservation splitting," in *Proc. IEEE Int. Conf. Connected Vehicles Expo (ICCVE)*, Nov. 2019, pp. 1–6.

[32] A. Gonzalez, N. Franchi, and G. Fettweis, "Control loop aware LTE-V2X semi-persistent scheduling for string stable CACC," in *Proc. IEEE 30th Annu. Int. Symp. Pers., Indoor Mobile Radio Commun. (PIMRC)*, Sep. 2019, pp. 1–7.

[33] A. D. Trabelsi, H. Marouane, F. Zarai, and A. Meddeb-Makhlouf, "Dynamic scheduling algorithm based on priority assignment for LTE-V2X vehicular networks," in *Proc. 15th Int. Wireless Commun. Mobile Comput. Conf. (IWCMC)*, Jun. 2019, pp. 483–488.

[34] Y. Wang, X. Zheng, and X. Hou, "A novel semi-distributed transmission paradigm for NR V2X," in *Proc. IEEE Globecom Workshops (GC Wkshps)*, Dec. 2019, pp. 1–6.

[35] A. Mansouri, V. Martinez, and J. Harri, "A first investigation of congestion control for LTE-V2X mode 4," in *Proc. 15th Annu. Conf. Wireless On-demand Netw. Syst. Services (WONS)*, Jan. 2019, pp. 56–63.

[36] A. Bazzi, "Congestion control mechanisms in IEEE 802.11p and sidelink C-V2X," in *Proc. 53rd Asilomar Conf. Signals, Syst., Comput.*, Nov. 2019, pp. 1125–1130.

[37] B. Toghi, M. Saifuddin, Y. P. Fallah, and M. O. Mughal, "Analysis of distributed congestion control in cellular vehicle-to-everything networks," in *Proc. IEEE 90th Veh. Technol. Conf. (VTC-Fall)*, Sep. 2019, pp. 1–7.

[38] R. Molina-Masegosa, J. Gozalvez, and M. Sepulcre, "Comparison of IEEE 802.11p and LTE-V2X: An evaluation with periodic and aperiodic messages of constant and variable size," *IEEE Access*, vol. 8, pp. 121526–121548, 2020.

[39] L. Lusvarghi and M. L. Merani, "On the coexistence of aperiodic and periodic traffic in cellular vehicle-to-everything," *IEEE Access*, vol. 8, pp. 207076–207088, 2020.

[40] A. Bazzi, G. Cecchini, M. Menarini, B. M. Masini, and A. Zanella, "Survey and perspectives of vehicular Wi-Fi versus sidelink cellular-V2X in the 5G era," *Future Internet*, vol. 11, no. 6, p. 122, May 2019.

[41] *Technical Specification Group Radio Access Network; Evolved Universal Terrestrial Radio Access (E-UTRA); Physical Layer Procedures; RElease 16*, Standard 3GPP TS 36.213 v16.3.0, 2010.

[42] A. Bazzi, C. Campolo, A. Molinaro, A. O. Berthet, B. M. Masini, and A. Zanella, "On wireless blind spots in the C-V2X sidelink," *IEEE Trans. Veh. Technol.*, vol. 69, no. 8, pp. 9239–9243, Aug. 2020.

[43] *Study on NR Vehicle-to-Everything (V2X); Release 16*, Standard 3GPP TR 38.885 v16.0.0, Mar. 2019.

[44] *Intelligent Transport Systems (ITS); Communications Architecture* Standard ETSI EN 302 665 v1.1.1, Sep. 2010.

[45] V. Martinez and F. Berens, "Survey on ITS-G5 CAM statistics," CAR 2 CAR Communication Consortium, Washington, DC, USA, Tech. Rep. TR2052, Dec. 2018.

[46] G. Cecchini, A. Bazzi, B. M. Masini, and A. Zanella, "LTEV2 Vsim: An LTE-V2 V simulator for the investigation of resource allocation for cooperative awareness," in *Proc. 5th IEEE Int. Conf. Models Technol. Intell. Transp. Syst. (MT-ITS)*, Jun. 2017, pp. 80–85.

[47] A. Bazzi, A. Zanella, I. Sarris, and V. Martinez, "Co-channel coexistence: Let ITS-G5 and sidelink C-V2X make peace," in *IEEE MTT-S Int. Microw. Symp. Dig.*, Nov. 2020, pp. 1–4.
[48] *Intelligent Transport Systems (ITS); Access Layer; Part 1: Channel Models for the 5, 9 GHz Frequency Band*, Standard ETSI TR 103 257-1 v1.1.1, May 2019.
[49] *Intelligent Transport Systems (ITS); Access Layer Specification for Intelligent Transport Systems Using LTE Vehicle to Everything Communication in the 5, 9 GHz Frequency Band*, Standard ETSI TS 103 613 v1.1.1, 2018.

STEFANIA BARTOLETTI (Member, IEEE) received the Laurea degree *(summa cum laude)* in electronics and telecommunications engineering and the Ph.D. degree in information engineering from the University of Ferrara, Italy, in 2011 and 2015, respectively.

She is currently a Researcher with the Institute of Electronics, Computer and Telecommunication Engineering (IEIIT) of the National Research Council of Italy (CNR) and an Associate Member of CNIT/WILAB. From 2016 to 2019, she was a Marie Skłodowska-Curie Global Fellow within the H2020 European Framework for a research project with the Massachusetts Institute of Technology and the University of Ferrara. Her research interests include theory and experimentation of wireless networks for localization and vehicular communications. She was a recipient of the 2016 Paul Baran Young Scholar Award of the Marconi Society. She has served as a Chair of the TPC for the IEEE International Conference on Communications Workshop on Advances in Network Localization and Navigation (ANLN) from 2017 to 2020. She is also an Editor of the IEEE COMMUNICATIONS LETTERS.

BARBARA MAVÌ MASINI (Senior Member, IEEE) received the Laurea degree *(summa cum laude)* in telecommunications engineering and the Ph.D. degree in electronic, computer science, and telecommunication engineering from the University of Bologna, Italy, in 2001 and 2005, respectively.

Since 2005, she has been a Researcher with the Institute for Electronics and for Information and Telecommunications Engineering (IEIIT) of the National Research Council (CNR). Since 2006, she has also been an Adjunct Professor with the University of Bologna. She works in the area of wireless communication systems and her research interests include connected vehicles, from physical and MAC levels aspects up to applications and field trial implementations. Her current research interests include relay assisted communications, energy harvesting, and visible light communication (VLC). She is currently a TPC member of several conferences, and a reviewer for most international journals and the Italian Ministry of Economic Development (MISE). She is also an Editor of *Computer Communication* (Elsevier). She was a Guest Editor of *Ad Hoc Networks* (Elsevier), Special Issue on Vehicular Networks for Mobile Crowd Sensing in 2015, *Mobile Information Systems*, Special Issue on Connected Vehicles: Applications and Communication Challenges in 2017, *Sensors*, Special Issue on Sensors Networks for Smart Roads in 2018. She is a Secretary of Chapter VT06/COM19 of the IEEE Italy section.

VINCENT MARTINEZ received the M.Sc. degree in mathematical and statistical modeling from INSA Toulouse, France.

He has been a Senior Principal Engineer with NXP Semiconductors (previously Freescale) since 2006. He is currently a Wireless Signal Processing and Physical Layer Expert, and is contributing to various V2X standardization bodies.

IOANNIS SARRIS received the B.Sc. degree in computing and physics from the University of Brighton, U.K., and the M.Sc. and Ph.D. degrees in wireless communications from the University of Bristol, U.K.

He is currently a Senior Principal Engineer with u-blox. His role involves the definition of V2X chipset architecture as well as the active contribution to the company's standardization and dissemination activities. He has previously held different positions in the company as a Senior Research Engineer and a Senior Manager of the DSP team involved with the development of a V2X chipset. Previously, he has worked for Mitsubishi Electric and Aircom International on research positions in wireless communications.

ALESSANDRO BAZZI (Senior Member, IEEE) received the Laurea degree and the Ph.D. degree in telecommunications from the University of Bologna, Italy, in 2002 and 2006, respectively. From 2002 to 2019, he was a Researcher of the National Research Council of Italy (CNR) and since the academic year 2006–2007, he holds courses at the University of Bologna in the area of wireless systems and networks. He is currently a Senior Researcher with the University of Bologna, and an Associate Member of CNIT/WILAB. His research interests include medium access control and radio resource management of wireless networks. Particular focus has been placed on connected and autonomous vehicles (CAVs), within national and international research projects. He is also a part of the ETSI Specialist Task Force on multi-channel operations. He delivered a keynote on CAVs at ICUMT2020, he won a Best Paper Award at ITSC 2017, he participated to several conferences as a tutorial instructor or a panelist (IARIA MOBILITY 2012, IEEE ISWCS2017, IEEE ComSoc Spring School 2019, and IEEE PIMRC 2019), and he organized Special Sessions or Workshops at IEEE PIMRC 2018 and IEEE PIMRC 2019. He is also in the Editorial Board of *Wireless Communications and Mobile Computing* (Hindawi) and *Vehicles* (MDPI), and the Chief Editor of *Mobile Information Systems* (Hindawi).